TITLE: Retrospective evaluation of thoracic computed tomography findings in dogs naturally infected by Angiostrongylus vasorum

AUTHORS: Mark E. Coia, Gawain Hammond, Daniel Chan, Randi Drees, David Walker, Kevin Murtagh, Janine Stone, Nicholas Bexfield, Lizzie Reeve, Jenny Helm

JOURNAL TITLE: VETERINARY RADIOLOGY & ULTRASOUND

PUBLISHER: Wiley

PUBLICATION DATE: 20 April 2017 (online)

DOI: 10.1111/vru.12505

RETROSPECTIVE EVALUATION OF THORACIC COMPUTED TOMOGRAPHY FINDINGS IN DOGS NATURALLY INFECTED BY ANGIOSTRONGYLUS VASORUM

Authors: Mark E. Coia[1], Gawain Hammond[1], Daniel Chan[2], Randi Drees[2], David Walker[3], Kevin Murtagh[4], Janine Stone[5], Nicholas Bexfield[6], Lizzie Reeve[7] and Jenny Helm[1].

Corresponding Author email: Jenny.Helm@glasgow.ac.uk

List of institutions:

1. University of Glasgow, School of Veterinary Medicine, College of Medical, Veterinary and Life Sciences, Bearsden, Glasgow, G61 1QH

Corresponding Author email jenny.helm@glasgow.ac.uk

2. Department of Clinical Science and Services, The Royal Veterinary College, Hawkshead Lane, North Mymms, Hatfield, Hertfordshire, AL9 7TA

3. Anderson Moores, The Granary, Bunstead Barns, Poles Lane, Hursley, Winchester, Hampshire, SO21 2LL

4. School of Veterinary Science, University of Liverpool, Leahurst Campus, Chester High Road, Neston, Wirral, CH64 7TE

5. Pride Veterinary Centre Riverside Road, Pride Park, Derby DE24 8HX

6. School of Veterinary Medicine and Science, University of Nottingham, Sutton Bonington Campus, Leicestershire, LE12 5RD

7. Langford Veterinary Services, University of Bristol, Langford House, Langford, Bristol, BS40 5DU

Key words: Canine, *Angiostrongylus vasorum*, computed tomography, CT, angiostrongylosis**.**

Running Head: Thoracic CT findings in dogs with natural *A. vasorum*

Abstract

Angiostrongylus vasorum (*A. vasorum*) is an important emerging disease of canidae. Cardiorespiratory signs are a common clinical manifestation in affected dogs, therefore thoracic imaging is critical in diagnosing and monitoring disease. Currently there is no description of thoracic computed tomography (CT) findings in dogs naturally infected with *A. vasorum*. The aim of this multicenter retrospective study was to review the findings on thoracic CT. Our goal was to identify any consistent changes, while standardizing the description of thoracic CT findings. Nine UK-based referral center's clinical and imaging databases were searched for cases, which had a confirmed diagnosis of *A. vasorum* and had undergone thoracic CT examination. Eighteen dogs, from seven of the centers, fulfilled the inclusion criteria. The lung lobes were divided into three zones and the CT changes described in each: pleural (zone 1), subpleural (zone 2) and peribronchovascular (zone 3). The prominent abnormality was increased lung attenuation due to poorly defined ground-glass opacity (GGO) or consolidation. There are regions of mosaic attenuation due to peripheral bronchiectasis. 50% dogs showed hyper attenuating nodules of varying sizes with ill-defined margins. The distribution always affected zone 1,2 with varied involvement of zone 3; this resulted in clear delineation between zones 2 and 3. Tracheobronchial lymphadenomegaly was frequently noted. This is the first study to provide information about CT findings in dogs naturally infected with *A. vasorum*. Findings are non-specific with considerable overlap with other pulmonary conditions, although the predominantly peripheral distribution means *A. vasorum* is the likely differential with such changes.

Abstract: 250

Word count: 4664

Introduction

Angiostrongylus vasorum (A. vasorum) is a nematodal endoparasite, belonging to the family Metastrongylidae, residing in the pulmonary arterial tree of domestic and wild canids. The nematode has a broad worldwide distribution including the United Kingdom (U.K.) and many regions of Europe with specific foci of clinical disease within endemic regions.[1-13] *A.vasorum* has been recognized as a cause of many significant disease processes, including but not limited to cardiopulmonary disease, coagulopathies and neurological disease.[4, 14-21] This array of clinical signs and the chronicity of the associated clinical signs may delay early detection and diagnosis of natural canine angiostrongylosis in a number of cases. Owing to the serious consequences of infection; disease is potentially fatal, there has been an increasing awareness over the past decade. The prognosis for infected patients varies, with an estimated mortality rate of 2-13% in a specialist referral facility despite appropriate treatment and intervention.[7, 15, 16, 22] As such, an early and accurate diagnosis is essential; this is possible owing to the laboratory methods that are readily available.

To date, clinical and experimental radiographic findings have been described in dogs with *A. vasorum;* radiographic findings are not pathognomonic for the interstitial pneumonia associated with the parasite. [23, 24] Thoracic Computed Tomography (CT) findings have only been reported in a series of six dogs experimentally infected with *A. vasorum*. The findings included a pronounced multifocal peripheral alveolar pattern in all the dogs. Additionally, there was evidence of nodular patterns and lung consolidation affecting areas of all lung lobes. Such findings are reported to be dependent on the parasitic burden induced experimentally. [25, 26] It was suggested in the experimental study that a method to compare the degree of pulmonary changes should be developed.

It is very possible that natural infection differs from experimental disease given that disease

in dogs can be chronic in nature, which may be associated with accumulative parasite numbers and the associated inflammatory reaction. Additionally, the timing of presentation for investigation will differ based on clinical signs and on owner/veterinarian observations. It is therefore unknown if the thoracic CT findings seen in experimentally infected dogs would be the same as those seen in dogs with natural infection presenting in a typical clinical setting on a less prescribed timeline. For this reason, there is a requirement to describe the imaging findings in naturally occurring infection of domestic canids.

To the authors' knowledge there is no literature describing the thoracic CT findings in a larger cohort of dogs naturally infected with *A.vasorum*. The aim of this multicenter retrospective study was to review the findings on thoracic CT in dogs naturally infected with *A. vasorum*. Our goal was to identify any consistent changes, while standardizing the description of thoracic CT findings. We hypothesized that the CT examination findings in naturally infected may correlate to the severity of the respiratory signs for each animal, and may differ to those described in experimental cases with acute infections and possibly higher worm burdens.

Materials and Methods

The study consisted of a retrospective review of the clinical records and thoracic CT sequences for all dogs diagnosed with angiostrongylosis at nine UK and Ireland-based referral centers, between 1st January 2010 and 1st July 2015 inclusively.

Each of the institutes' clinical and imaging databases were searched for cases that would fulfill the study criteria; using any of the keywords "*Angiostrongylus vasorum A. vasorum,* angiostrongylosis, lungworm, thoracic CT, parasitic pneumonia, and/or verminous"

The following were inclusion criteria for this study:

(1) A confirmed diagnosis of *A. vasorum* using at least one of the following modalities: faecal smear, Baermann examination with morphological identification, bronchoalveolar lavage (BAL), point- of care ELISA test (Angiodetect™*), polymerase chain reaction (PCR), antibody detection, or laboratory verified antigen detection.

(2) Complete clinical notes and the owners' permission for their dogs to be included in the study.

(3) Full thoracic CT scan (helical).

(4) The absence of previous diseases that could result in thoracic CT changes (e.g. congestive heart failure, or evidence of disseminated neoplasia). Ancillary tests utilised included but were not limited to; BAL, bronchoscopy, biochemistry, haematology, echocardiography and coagulation profiles. A positive diagnosis of *A. vasorum* was therefore identified as the aetiological cause for the clinical manifestations in each case.

Data recorded from the files included breed, gender, date of birth, number of dogs in household, travel history, concurrent disease(s), concurrent medication, associated clinical signs, laboratory data, CT and radiographic findings and clinical outcome of the dogs. The presence or absence of respiratory signs (cough, tachypnea and dyspnea) were identified and if present, was noted as having an acute or chronic onset.

The dogs were grouped as juvenile (0-1 years), adult (1-6 years), or mature (6+ years) to assess if age or life-stage affected the severity of the radiological changes on thoracic CT. Categorization of their life stage was applied based on previously published criteria.[27]

CT studies of the full thorax were acquired with the patients under general anesthesia or sedation using different third generation CT units† in helical scan mode. Similar protocols were used between the institutions including a high-and medium frequency spatial reconstruction algorithm, high kV (120-130) and appropriate mAs, patient size adjusted

display field of view (FoV), pitch (0.8-1.8) and high-resolution reconstruction filters. Images were reconstructed at 0.5-5.0 mm slice thickness (Table 1). Where contrast was administered, an intravenous infusion of iodinated contrast medium‡ was administered via an indwelling intravenous cannula placed in the cephalic or saphenous veins at a dose of 2mL/kg. The dogs were placed in sternal or right lateral recumbency for acquisition of the CT sequences. All dogs under general anaesthesia were ventilated as per the facilities breath hold protocols, thus minimising atelectasis and motion artefact during acquisition.

The CT studies were reviewed independently by board-certified diagnostic imaging staff at each referral center at the time of diagnosis, followed by a standardized retrospective assessment by a board-certified radiologist (GH). The retrospective CT analysis was performed using a dedicated digital imaging and communications in medicine (DICOM) workstation (Visbion Image viewer) § in both soft tissue and lung algorithms, with the window width (WW) and window level (WL) adjusted as required. During the retrospective analysis, the radiologist was aware that all patients had a diagnosis of angiostrongylosis, but was blinded to the severity of the presenting signs and other patient information.

The individual findings for each CT were classified based on the predominating pulmonary patterns. Pulmonary CT changes were classified as per a previously described system for the assessment of CT findings of the canine lungs, after being adapted from human medicine.[25, 28-31] The lungs were divided into three zones: Zone 1, which is the pleural region, describes the 1mm area around the periphery of each lung lobe. Zone 2, which is the subpleural region of the lungs, describes the 5 per cent of the maximum lobar width of the lung parenchyma lying beneath the visceral pleura; Zone 3, defined as the peribronchovascular region contains the peribronchovascular interstitium that surrounds the central bronchi and pulmonary

arteries, extends into the peripheral lung and incorporates the remaining lung that is not already included within the pleural and subpleural zones.

The lobes affected were described as single lobe, multiple lobes unilaterally or multiple lobes bilaterally. Pleural changes were defined as the capability to identify the pleura or pleural space on the images; such changes recorded could consist of 'pleural thickening'; 'enhancement'; or 'effusion'.[32, 33]

Abnormalities affecting each zone were further divided into the following categories: (a) linear and reticular; (b) nodules and nodular; (c) high attenuation: ground – glass opacification (GGO), consolidation, atelectasis and mineralization; (d) low attenuation: air trapping or cystic lesions (honeycombing, cysts, bullae, bronchiectasis and emphysema); (e) mosaic attenuation pattern- this appears as a patchwork of regions in different attenuation suggesting interstitial changes. CT findings for each dog were given a severity score: mild (1), moderate (2) and severe (3) which was assigned by our board certified diagnostic imager (Table 2). Additionally, other criteria included: lung lesions (solitary, lobar, diffuse, multifocal); number of lung lobes involved; vasculature changes (tortuous or thrombi) and tracheobronchial lymphadenopathy. The pulmonary arterial diameter was compared to the accompanying bronchi, using the bronchoarterial ratio (BA Ratio).[34, 35] The main pulmonary artery to aortic diameter ratio (MPA:Ao) was measured for each dog using CT measurements in the soft tissue window, to assess for presence of pulmonary hypertension. The MPA:Ao was assessed as previously described in the veterinary literature with a window level of 40HU and window width of 350HU.[36]

Contrast enhancement of any lesion(s) was evaluated for homogenous or heterogeneous uptake. Summary statistics were performed. The relevant Ethics and Welfare committees granted approval for the retrospective study prior to publication.

Results

Seven of the nine centers[¶] in the UK provided cases, following determination of suitability. Twenty dogs (20) were originally identified; however, two dogs (2) were excluded, as they did not fulfill the inclusion criteria. Therefore, eighteen dogs (18) with confirmed canine angiostrongylosis were included in this study. 17/18 dogs were anaesthetized for CT exam; 1/18 dog was sedated for the imaging. 17/18 dogs were placed in sternal recumbency and 1/18 placed in right lateral for acquisition of the scans. All eighteen dogs had a diagnosis established within 5 days of the CT imaging.

All dogs recovered uneventfully following the procedure. A contrast agent was administered in (11/18) animals (as described earlier); no complications were associated following administration of the agent in any dog. The dogs ranged in age from 6 months to 12 years 4 months; the median age was 7 years 3 months. Gender distribution was 6/18 male entire (33%), 4/18 male neutered (22%), 3/18 female entire (17%) and 5/18 female neutered (28%). The clinical signs of the 18 dogs included: acute respiratory distress in 61% (11/18); exercise intolerance in 50% (9/18); coughing in 44% (8/18); bleeding diathesis (3/18), neurological (3/18) and weight loss (3/18) in 16.7% and pyrexia was noted in 11% of dogs (2/18). 3/18 dogs had the absence of respiratory signs and were presented for the investigation of bleeding diathesis or neurological assessment. The reader is invited to refer to the further demographic results and clinical findings of the population which are shown in Appendix 1.

Bronchoscopy was undertaken and a bronchoalveolar lavage conducted as part of the initial investigations in 15/18 dogs. Cytological examination of the bronchoalveolar lavage shows a mixed inflammatory cell population (13/15), isolation of angiostrongylus larvae (10/15), pyogranulomatous inflammation on lung aspirates (2/15) and a positive culture for Pasteurella sp. and E. coli sp. (2/15). Fourteen (14) cases had non-specific changes on blood biochemical analysis. Hematological changes were observed in 12/18 animals, with

225 eosinophilia, anemia and monocytosis being the most frequently observed anomalies. Other
226 changes included thrombocytopenia and neutrophilia. Of the three cases presented for a
227 suspected coagulopathy only two had detectable changes: one with prolonged activated
228 partial thromboplastin time (APPT) and the other had altered platelet function identified
229 using the multiplate analyzer.[‖]
230 The dogs were treated as follows: fenbendazole (11/18), imidacloprid /moxidectin (2/18) or a
231 combination of fenbendazole and imidacloprid /moxidectin (5/18). Various supportive
232 medications were given prior to CT examination, these included corticosteroids, theophylline
233 and broad-spectrum antibiotics. The time between onset of clinical signs and CT examination
234 varied in each dog from days to two weeks. Treatment with supportive therapy and
235 anthelmintic led to complete resolution of the clinical signs in thirteen cases (13/18), while
236 clinical response was unknown in four cases. One patient's respiratory signs resolved with
237 the treatment given, however later this dog was euthanized for unknown reasons at the
238 owner's request.
239
240 All dogs (18/18) demonstrated evidence of lung lesions on CT, located within the right
241 cranial, caudal, accessory, and left caudal lobes; the right middle and left cranial lobes were
242 affected in 16/18 dogs. All dogs had increased attenuation within the pleural region (zone 1)
243 (18/18). These severely affected regions lay within the dorsal, mid and ventral aspects of the
244 lungs; the dorsal and ventral aspects are most severely affected (16/18). The most notable
245 feature identified within the subpleural region (zone 2) was a multifocal to diffuse increase in
246 lung attenuation in fourteen dogs. There was obvious dorsal or ventral predilection noted on
247 the CT examinations. On the CT images the main findings affecting the peribronchovascular
248 region (zone 3) was an increased attenuation of the parenchyma in 15/18 dogs. The changes
249 noted within zone 3 of the lungs appear to be an extension from zone 2 (7/18) and multifocal

/ diffuse in the other cases. The caudal lobes were severely affected by this peribronchovascular distribution (11/18), with a multifocal distribution affecting all lobes (4/18) or individual lobes (3/18). In severe cases (6/18), there was mosaic attenuation of poorly circumscribed GGO to consolidation. Additionally, mild to moderate bronchiectasis (6/18) was diffusely noted and there was subtle subjective peribronchovascular thickening (peribronchial cuffing).

Zone 1 demonstrated multifocal linear and reticular patterns with parenchymal bands, extending from the visceral pleura, in 14/18 cases (Fig. 1A, B). The most notable feature identified zone 2 was a multifocal to diffuse increase in lung attenuation suggestive of poorly circumscribed GGO in fourteen dogs (14/18), with base wide wedge-shaped areas of consolidation noted in these cases; these appear widest towards the periphery of each lobe (15/18) (Fig.2A, B). Ill-defined hyper-attenuating nodules ranging in size from small (3mm) to large (85mm) were observed throughout the parenchyma with a random distribution (9/18); no obvious dorsal or ventral predilection was noted (Fig.3A, B). All nodules had hazy margins with heterogeneous attenuation on unenhanced lung window (HU: -136 to HU:36). On the CT examinations, the main findings affecting zone 3 was an increased attenuation of the parenchyma with a generalized admixed consolidation (15/18) and GGO (15/18).

Additional CT findings include moderate tracheobronchial lymph node enlargement (16/18), mild to moderate cranial mediastinal lymphadenomegaly (6/18), cardiomegaly (1/18) and pneumomediastinum (1/18). There was evidence of pulmonary arterial dilation in four dogs (4/18) with a reduction in BA ratio of 1.1, 1.3, 1.1, 1.12 respectively. Six dogs exhibited an increased BA ratio, these were: 1.6, 1.66, 1.75, 1.77, 1.77, 2.1 respectively. The mean BA

ration in the eighteen dogs was 1.44. The MPA:Ao measurement was similar in eighteen dogs, with a mean of 1.02 and median value of 0.99. There was no evidence of pleural effusion noted in any of the cases reviewed in this series. Mild to moderate bronchiectasis was noted (6/18) with moderate to severe CT changes. The bronchiectasis was diffusely noted. There was evidence of small to medium sized airways extending to the periphery of the lung lobes (zone 2) without apparent tapering in diameter, supportive of bronchiectasis (6/18). These small airways were visualized at the periphery – surrounded by GGO or consolidation.

Discussion

The CT findings in this study were comparable, yet not identical to those observed in dogs with both low-grade and high-grade experimental infections.[25] Dogs naturally infected with *A. vasorum* demonstrated the following CT features, predominately a diffuse to multicentric, increased lung attenuation, affecting multiple lobes. In addition, these dogs developed a marked consolidation in the ventral aspect of the lobes of soft tissue attenuation; as in the previous study. Thoracic CT was conducted in all eighteen dogs to facilitate investigation of respiratory signs or to further assess for systemic or neoplastic/ metastatic disease responsible for the clinical manifestations. Pulmonary changes were detected on CT for all eighteen dogs, despite the lack of respiratory signs in three dogs at the time of presentation. These three dogs demonstrated mild to moderate pulmonary changes on CT examination (severity score 1-2). This was not supportive of the hypothesis in this study; the severity of the respiratory signs did not relate to the imaging findings on CT.

The previous study conducted in beagles showed a moderate, multicentric GGO with nodule formations of varying sizes and consolidated regions of the lungs; these regions of

consolidation were well demarcated with a geometric appearance resembling a wedge shape. The region of consolidation was widest towards the periphery of the lungs. The high-grade infected dogs demonstrated severe changes; which were comparable to the low-grade infected group but more profound. The documented findings included large, coalescing nodules with larger areas of consolidation. These affected areas were surrounded by a rim of GGO. The dogs with high-inoculated levels of the parasite developed pleural fissure signs suggestive of effusion or pleuritic, this was not seen in this study of naturally infected dogs In the previous study, all dogs had prominence of the regional lymph nodes (tracheobronchial, mediastinal and retrosternal) suggestive of lymphadenomegaly. The tracheobronchial lymphadenomegaly noted in the previous literature was not a consistent finding in this study of naturally infected dogs, but (16/18) of the dogs did demonstrate tracheobronchial lymph node enlargement. There was normal attenuation and tapering of the pulmonary vasculature in the experimental study, however the pulmonary arteries close to the nodules and wedge shaped parenchymal changes demonstrated filling defects. These changes were interpreted as intra luminal thrombi secondary to the parasitic infestation. We could identify similar changes on retrospective analysis of CT imaging, while quantitatively and descriptively documenting the location and type of changes in each dog.

Zone 1 demonstrated heightened attenuation; such findings may be suggestive of pleural thickening or a small volume of effusion, which was a consistent finding in all cases. The parenchymal bands, seen as non-tapering, reticular hyperattenuating opacities, that extend from the visceral pleural (zone 1) may be the result of fibrosis and thickening of the interstitial fiber network of the lung periphery. The changes may suggest fluid, fibrous tissue or interstitial cellular infiltration, but would require histopathology to correlate the findings.[37, 38]

The GGO in the peripheral regions of the lungs (zone 2) may be the result of thickening of subpleural interstitium, or inflammatory cell infiltrates within the interstitium or alveolar air space, thus resulting in consolidation. The peripheral lung changes are likely to be associated with multiple granulomatous lesions centered around the margination of parasite eggs and larvae of A. vasorum in the periphery at the lung capillaries. The alveolar changes may be the result of the L1 larvae moving into the alveoli and smaller bronchioles. The lifecycle of this nematode (namely the eggs and L1 larvae) are likely responsible for the distribution observed.[38, 39]

The dogs in our study did not have convincing intraluminal filling defects but there were changes suggestive of pulmonary arterial dilation. Despite the objective assessment for pulmonary hypertension, the MPA:AO ratios were interpreted as normal. The study that had looked at reference ranges for MPA:Ao was based on a small cohort of ten dogs, each being described as clinically well. It was therefore not certain if a reference range can be extrapolated from the results, however, a ratio of >1.1 may be interpreted as being normal when calculated from CT measurements in healthy dogs. The reliability of this measurement to deduce if a dog is suffering from pulmonary hypertension is uncertain. To date, echocardiography is described as a reliable and non-invasive method to estimate pulmonary arterial parameters that can be used to deduce if pulmonary arterial hypertension (PAH) is present. Overemphasis of one parameter or measurement could be undependable, when interpreting any imaging study. Measurements extrapolated from imaging can easily be over utilized in a clinical setting. A complete assessment for PAH includes evaluation of the pulmonary vasculature, cardiac evaluation, and evaluation of lung parenchyma. The identification of several anomalies will provide support for reliably diagnosing pulmonary

hypertension.[36, 40-42] Towards the periphery it was difficult to observe the smaller pulmonary arteries due to effacement resulting from the increased attenuation. Therefore, filling defects and thrombi may be easily overlooked. Subjective bronchiectasis was observed, however only one dog has BA ratio > 2 which would be conclusive for bronchiectasis. There is evidence of dilated, blunt ending airways extending into the periphery of the lung parenchyma (zone 2) resulting in a mixed attenuation (mosaic). Such findings should not be observed in the normal canine lungs; this may be associated with chronic pathology and fibrosis resulting in traction bronchiectasis.

The nodules that were observed had a random distribution, with ill-defined margins. The attenuation was not solely soft tissue and resembled that of GGO, therefore was suggestive of an admix of air and fluid.

The immunopathogenesis of canine angiostrongylosis is reported: deposits of immunoglobulins, complement and fibrinogen have been detected in the lungs of affected dogs. This inflammatory response is proposed to be caused by the migration of larvae throughout pulmonary tissue and leads to multifocal granulomatous pneumonia (with variable amounts of suppurative and eosinophilic inflammation). In some cases, the migrating larvae crossing into the airspace of the alveoli result in pulmonary hemorrhage. [1, 3-5, 11, 12, 21, 38, 43-45]

One case showed signs consistent with pneumomediastinum, which can be associated with bronchial, tracheal or alveolar pathology (most notably rupture). Spontaneous pneumomediastinum has been noted in greyhounds without associated clinical signs. In such cases the source of the gas is often obscure.[46] Since the affected dog was a greyhound, the significance of this finding is unknown and may be incidental.

375 Notably, the ventral aspects of the lung lobes were severely affected in 16/18 dogs; equally,
376 this was identified in a previous study. The distribution was believed to relate to pathology
377 resulting in consolidation, due to the characteristics and extent of the changes on CT.

378 Our goal was to identify any consistent changes on the CT examinations. Such findings and
379 distribution of the lesions are highly suggestive of *A. vasorum;* however, differential
380 diagnosis of the heterogeneous hyper-attenuating pulmonary nodules and ground glass
381 opacity include eosinophilic bronchopnemopathy, pulmonary lymphoma, granulomatous lung
382 disease and intrathoracic histiocytic sarcoma.[32, 40-42, 47]
383 It has been suggested that younger dogs (often under the age of eighteen months) are more
384 likely to show clinical manifestations following infection with *A. vasorum*, with the highest
385 proportion of dogs under the age of eighteen months. This occurrence in younger animals
386 could be attributed to age-related tendencies and behavior, or incomplete immunity. [3, 15, 48 48,
387 49] The majority of cases in our study, albeit a small population, were adults (5/18) or mature
388 adults (11/18), which did not reflect the distribution noted in previous studies.[15, 16] The
389 difference in distribution of age observed in our group of dogs could relate to older animals
390 being immune-compromised due to factors such as concurrent infection or disease (although
391 there was no evidence for this), or they may be immune-naïve if the parasite has recently
392 emerged in that area. A lack of owner awareness of clinical signs and inadequate
393 prophylactic anthelmintic control may also result in significant parasitic burdens in areas
394 recently colonised by the parasite. It's possible that the parasitic burden may be
395 accumulative with time, resulting in higher burdens in older animals. Additionally, some of
396 the younger patients may have presented with acute or pathognomonic clinical signs at a
397 primary care facility and may have been treated earlier, thus not requiring investigations at a
398 referral level, or requiring a thoracic CT for further investigation. From a diagnostic imaging
399 viewpoint, the age distribution seen in this study means that metastrongyloid disease should

appear on differential lists when similar CT findings are reported, even when the age demographic makes other differentials (such as neoplasia) seem more likely.

Due to the limited number of cases, summary statistics were conducted and the findings are purely descriptive. The involvement of seven referral centres allowed for increased enrolment of cases, however this meant that the thoracic CT studies were acquired in different facilities. As such, there was reduced capability for standardisation of the CT scan protocols. Although the thoracic CT was conducted within 14 days of a diagnosis with *A. vasorum*, there may have been delayed diagnosis, meaning that each animal may have been at a different stages of disease progression. A single board-certified radiologist reviewed the images to improve standardisation of the descriptive terms. The radiologist was not blinded to the clinical diagnosis when analysing the sequences. Atelectasis, whether passive, compressive or cicatrisation should be considered at least as a contributing cause for this distribution of abnormalities within the lungs. Owing to the general anesthesia and sternal positioning for acquisition of the CT exam, passive atelectasis is likely where there is a decreased lung volume. General anesthesia may result in notable alterations in aeration and may need to increased opacity of the lungs in the dependent lung fields. Unfortunately, atelectasis can prove difficult to eliminate, especially during prolonged procedures. Where radiographs were taken as part of the investigation, they were conducted on a previous day, thus to minimize general anesthesia and positioning artefacts. CT examinations are routinely conducted prior to procedures to minimize incomplete expansion of the lungs and development of atelectasis. By convention, all centers conducted a single breath hold protocol prior to the CT, usually with a positive pressure of 15-20cmH_2O. This was conducted for more consistent lung inflation and to reduce motion artefact. One dog (1/18)

presented with acute dyspnea, the dog was placed in right lateral recumbency for acquisition of the study because its respiratory signs were improved in this position.

A diagnosis of *A.vasorum* was reached following a positive result using at least one ancillary test, while showing compatible symptoms. BAL was conducted in fifteen dogs (15/18); the results were used to assess for underlying airway disease. There are limitations relating to the cytological analysis of fluid and fine-needle aspirates of lung lesions may reflect the cells and pathology more accurately. [50] It should be noted that ideally all dogs would have been screened for underlying lung pathology using bronchoscopy and BAL examination, however this was not clinically indicated in the three dogs without respiratory signs. The clinical significance of a positive bacterial culture of the BAL fluid documented in two dogs is unknown. The pathogenesis of the bacteria cannot be fully identified, however is has been shown that coinfection by parasitic and bacterial infections do occur in a number of dogs.[3] It is therefore difficult to assimilate which findings may be attributed to a bacterial bronchopneumonia or the verminous pneumonia. Many of the dogs (16/18) were provided with symptomatic treatment (not including appropriate anthelmintic; Four dogs received corticosteroids, nine dogs received antimicrobials and four dogs were given furosemide) in a primary care setting, prior to further investigations. It is difficult to objectively assess how pharmaceutical administration may affect BAL or CT examination findings. This is certainly a limitation of the study.

A future prospective study may include a panel of radiologists, who are blinded to the clinical diagnosis, with the inclusion of cases with alternative pulmonary pathology, such as lymphoma, acute respiratory distress syndrome and other causes of non-cardiogenic pulmonary oedema, allowing for comparisons of the description of the findings and distribution. Additionally, it would be beneficial to acquire repeat thoracic CT images

following successful treatment; allowing for identification of any long-standing changes that may alter prognostication. Follow up thoracic CT sequences were not performed on the dogs in this study; this may be due to various reasons, including clinical improvement of the dogs without a clinical rational to do so. There is interest in quantitative assessment of pulmonary pathology in human medicine and radiology, this could be an avenue explored to further objectify these findings.

This study is the first to provide information about the thoracic CT findings in naturally infected *A. vasorum* dogs that demonstrated various clinical manifestations. In conclusion, canine angiostrongylosis results in pulmonary changes in all patients with mild to moderate lymphadenomegaly. While successfully able to document the distribution and extent of the abnormalities, the findings observed on CT of naturally infected dogs may take various appearances and they are non-specific with a considerable overlap with other pulmonary conditions. Although the predominant findings described in this study were a peripheral distribution of increased lung attenuation with diffuse, poorly organized and multifocal nodules that are of GGO. The findings in this study echoed those reported on CT examination of six dogs experimentally infected with *A.vasorum*, yet they were not identical. It appears that the absence of respiratory signs does not denote the degree of changes on CT examination and initial presenting manifestations do not signify the anticipated degree of changes on thoracic CT.

List of Author Contributions

Category 1

(a) Conception and Design

Jenny, Mark, Gawain

(b) Acquisition of Data

ALL

(c) Analysis and Interpretation of Data

Jenny, Mark, Gawain

Category 2

(a) Drafting the Article

ALL

(b) Revising Article for Intellectual Content

ALL

Category 3

(a) Final Approval of the Completed Article

ALL for this version

Acknowledgements

The authors would like to thank all staff at the centers that took part in this study; including those that did not have cases that fulfilled the strict inclusion criteria.

References

1. Bolt, G., et al., The common frog (Rana temporaria) as a potential paratenic and intermediate host for Angiostrongylus vasorum. Parasitol Res, 1993. 79(5): p. 428-30.
2. Helm, J.R., et al., A case of canine Angiostrongylus vasorum in Scotland confirmed by PCR and sequence analysis. J Small Anim Pract., 2009. 50(5): p. 255-259.
3. Morgan, E.R., et al., Angiostrongylus vasorum infection in dogs: Presentation and risk factors. Vet Parasitol, 2010. 173(3-4): p. 255-61.
4. Morgan, E.R., et al., Angiostrongylus vasorum: a real heartbreaker. Trends Parasitol., 2005. 21(2): p. 49-51.
5. Morgan, E.R. and A.H.S. Tomlinson, Nichols T, Roberts E, Fox MT, Taylor MA., Angiostrongylus vasorum and Eucoleus aerophilus in foxes (Vulpes vulpes) in Great Britain. Vet Parasitol, 2008. 154(1-2): p. 48-57.
6. Morgan, E.R., et al., Canine pulmonary angiostrongylosis: the influence of climate on parasite distribution. Parasitol Int, 2009. 58(4): p. 406-10.
7. Helm, J.R., et al., Canine angiostrongylosis: an emerging disease in Europe. J Vet Emerg Crit Care (San Antonio), 2010. 20(1): p. 98-109.
8. Conboy, G.A., Canine angiostrongylosis: the French heartworm: an emerging threat in North America. Vet Parasitol, 2011. 176(4): p. 382-9.
9. Jolly, S., et al., First report of a fatal autochthonous canine Angiostrongylus vasorum infection in Belgium. Parasitol Int, 2015. 64(1): p. 97-9.
10. Helm, J.R., et al., Epidemiological survey of Angiostrongylus vasorum in dogs and slugs around a new endemic focus in Scotland. Vet Rec., 2015. 10.1136/vr.103006: p. 1-6.
11. Bourque, A.C., et al., Pathological findings in dogs naturally infected with Angiostrongylus vasorum in Newfoundland and Labrador, Canada. J Vet Diagn Invest, 2008. 20(1): p. 11-20.

12. Bourque, A., et al., Angiostrongylus vasorum infection in 2 dogs from Newfoundland. Can Vet J, 2002. 43(11): p. 876-879.
13. Traversa, D., A.M. Torbidone, D., and C. Guglielmini, Occurrence of fatal canine Angiostrongylus vasorum infection in Italy. Vet Parasitol, 2008. 152(1-2): p. 162-166.
14. Yamakawa, Y., et al., Emerging canine angiostrongylosis in northern England: five fatal cases. Vet Rec., 2009. 164(5): p. 149-152.
15. Chapman, P.S., et al., Angiostrongylus vasorum infection in 23 dogs (1999–2002). J Small Anim Pract., 2004. 45(9): p. 435-440.
16. Koch, J. and J.L. Willesen, Canine pulmonary angiostrongylosis: an update. Vet J., 2009. 179(3): p. 348-359.
17. Ramsey, I.K., et al., Role of chronic disseminated intravascular coagulation in a case of canine angiostrongylosis. Vet Rec., 1996. 138(15): p. 360-363.
18. Cury, M.C., et al., Western blot analysis of the humoral response of dogs experimentally infected with Angiostrongylus vasorum (Baillet, 1866). Vet Parasitol, 2002. 106(1): p. 83-87.
19. Cury, M.C., et al., Hematological and coagulation profiles in dogs experimentally infected with Angiostrongylus vasorum (Baillet, 1866). Vet Parasitol, 2002. 104(1): p. 139-149.
20. Cury, M.C., et al., Biochemical serum profiles in dogs experimentally infected with Angiostrongylus vasorum (Baillet, 1866). Vet Parasitol, 2005. 128(1-2): p. 121-127.
21. Traversa, D., A. Di Cesare, and G. Conboy, Canine and feline cardiopulmonary parasitic nematodes in Europe: emerging and underestimated. Parasit Vectors, 2010. 3(62): p. 1-22.

22. Willesen, J.L., et al., Efficacy and safety of imidacloprid/moxidectin spot-on solution and fenbendazole in the treatment of dogs naturally infected with Angiostrongylus vasorum (Baillet, 1866). Vet Parasitol, 2007. 147(3-4): p. 258-264.
23. Boag, A.K., et al., Radiographic findings in 16 dogs infected with Angiostrongylus vasorum. Vet Rec., 2004. 154(14): p. 426- 430.
24. Mahaffey, M.B., et al., Experimental canine angiostrongylosis: II. Radiographic manifestations. . J Am Anim Hosp Assoc, 1981. 17: p. 499-502.
25. Dennler, M., et al., Thoracic computed tomography findings in dogs experimentally infected with angiostrongylus vasorum. Vet Radiol Ultrasound, 2011. 52(3): p. 289-294.
26. Kinns, J., et al., Special Software Applications. In: Schwarz T, Saunders J (eds): Veterinary Computed Tomography. Wiley-Blackwell., 2011: p. 67-74.
27. Bartges, J., et al., AAHA canine life stage guidelines. J Am Anim Hosp Assoc, 2012. 48(1): p. 1-11.
28. Johnson, V.S., et al., Thoracic high-resolution computed tomographic findings in dogs with canine idiopathic pulmonary fibrosis. J Small Anim Pract., 2005. 46(8): p. 381-8.
29. Johnson, V.S., et al., Thoracic high-resolution computed tomography in the diagnosis of metastatic carcinoma. J Small Anim Pract., 2004. 45(3): p. 134-43.
30. Webb, W.R., N.L. Muller, and D.P. Naidich, Technical aspects of high-resolution computed tomography, normal lung anatomy. In: High resolution CT of the Lung, 3rd edn. McLaughlin. Lippincott, Williams and Wilkins, Philadelphia, 2001: p. 1-71.
31. Ohlerth, S. and G. Scharf, Computed tomography in small animals--basic principles and state of the art applications. Vet J, 2007. 173(2): p. 254-71.
32. Reetz, J.A., E.L. Buza, and E.L. Krick, CT features of pleural masses and nodules. Vet Radiol Ultrasound, 2012. 53(2): p. 121-7.

33. Wisner, E.R. and A.L. Zwingenberger, Pleural space In: Wisner E.R and Zwingenberger A.L. (eds): Atlas of Small Animal CT and MRI, 1st edn. Wiley-Blackwell., 2015: p. 398-407.

34. Cannon, M.S., et al., Computed tomography bronchial lumen to pulmonary artery diameter ratio in dogs without clinical pulmonary disease. Vet Radiol Ultrasound, 2009. 50(6): p. 622-4.

35. Schwarz, T. and V. Johnson, Lungs and Bronchi. In: Schwarz T. and Saunders J.H. (eds). Veterinary Computed Tomography. Wiley-Blackwell., 2011. 1st ed.: p. 261-278.

36. Granger, L.A., et al., Computed Tomographic Measurement of the Main Pulmonary Artery to Aortic Diameter Ratio in Healthy Dogs: A Comparison to Echocardiographically Derived Ratios. Vet Radiol Ultrasound, 2016. 57(4): p. 376-86.

37. Webb , W.R., N.L. Muller, and D.P. Naidich, High- Resolution Computed Tomography Findings of Lung Disease. In: Webb N.R (eds). High-resolution CT of the Lung. Lippincott Williams & Wilkins, 2008. 4th ed: p. 65 - 176.

38. Rinaldi, L., et al., Angiostrongylus vasorum: epidemiological, clinical and histopathological insights. BMC Vet Res, 2014. 10: p. 236.

39. Zarelli, M., et al., Imaging diagnosis: CT findings in a dog with intracranial hemorrhage secondary to angiostrongylosis. Vet Radiol Ultrasound, 2012. 53(4): p. 420-3.

40. Fina, C., et al., Computed tomographic characteristics of eosinophilic pulmonary granulomatosis in five dogs. Vet Radiol Ultrasound, 2014. 55(1): p. 16-22.

41. Tsai, S., et al., Imaging characteristics of intrathoracic histiocytic sarcoma in dogs. Vet Radiol Ultrasound, 2012. 53(1): p. 21-7.

42. Mesquita, L., et al., Computed tomographic findings in 15 dogs with eosinophilic bronchopneumopathy. Vet Radiol Ultrasound, 2015. 56(1): p. 33-9.

43. Patterson-Kane, J.C., L.M.J. Gibbons, R. Morgan, E.R., and N.R. Wenzlow, S.P., Pneumonia from Angiostrongylus vasorum infection in a red panda (Ailurus Fulgens Fulgens). J Vet Diagn Invest, 2009. 21(2): p. 270-3.

44. Simpson, V.R., Angiostrongylus vasorum infection in foxes (Vulpes vulpes) in Cornwall. Vet Rec., 1996. 139(18): p. 443-445.

45. Verzberger-Epshtein, I., et al., Serologic detection of Angiostrongylus vasorum infection in dogs. Vet Parasitol, 2008. 151(1): p. 53-60.

46. Jones, B.R., M.L. Bath, and A.K. Wood, Spontaneous pneumomediastinum in the racing Greyhound. J Small Anim Pract, 1975. 16(1): p. 27-32.

47. Geyer, N.E., et al., Radiographic appearance of confirmed pulmonary lymphoma in cats and dogs. Vet Radiol Ultrasound, 2010. 51(4): p. 386-90.

48. Di Cesare, A. and D. Traversa, Canine angiostrongylosis: recent advances in diagnosis, prevention, and treatment. Veterinary Medicine: Research and Reports, 2014. 5(2014): p. 181-192.

49. Barutzki, D. and R. Schaper, Natural infections of Angiostrongylus vasorum and Crenosoma vulpis in dogs in Germany (2007-2009). Parasitol Res, 2009. 105 Suppl 1: p. S39-48.

50. DeBerry, J.D., et al., Correlation between fine-needle aspiration cytopathology and histopathology of the lung in dogs and cats. J Am Anim Hosp Assoc, 2002. 38(4): p. 327-336.

Footnotes:

*IDEXX Europe B.V. P.O. Box 1334 NL -2130 EK Hoofddorp, The Netherlands

†CT Units: Siemens Dual Slice Somatom Spirit, Siemens AG, Arlangen, Germany;
GE Medical HighSpeed CT/e Dual, GE Medical Systems, Milwaukee, WI

; GE Medical Brightspeed, GE Medical Systems, Milwaukee, WI

; Philips MX8000 IDT 16, Philips Medical Systems, 5680 DA Best The Netherlands; Toshiba Aquilion Prime, Toshiba Medical Systems Europe B.V. Zoetermeer, The Netherlands; Siemens Emotion 16, Siemens AG, Arlangen, Germany

‡Contrast medium: XENETIX 300mg I/ml (Iobitridol) solution for IV injection, Guerbet, France; Omnipaque 300mg I /ml (iohexol) solution for IV injection, GE Healthcare, Princeton, NJ 08540 U.S.A.

§Visbion Image viewer, Visbion, Visbion House, Surrey, UK

‖Multiplate analyser™: Roche Diagnostics International Ltd CH-6343 Rotkreuz, Switzerland

¶*Institutes involved: The University of Glasgow,* Small Animal Hospital, School of Veterinary Medicine, College of Medical, Veterinary and Life Sciences, Bearsden, Glasgow, G61 1QH*; The Royal Veterinary College,* Hawkshead Lane, North Mymms, Hatfield, Hertfordshire, AL9 7TA*; Anderson Moores,* The Granary, Bunstead Barns, Poles Lane, Hursley, Winchester, Hampshire, SO21 2LL**;** *University of Liverpool, School of Veterinary Science*, Leahurst Campus, Chester High Road, Neston, Wirral, CH64 7TE; *Pride Veterinary Centre,* Riverside Road, Pride Park, Derby DE24 8HX; *School of Veterinary Medicine and Science, University of Nottingham*, Sutton Bonington Campus, Leicestershire, LE12 5RD**;** *University of Bristol, Langford Veterinary Services,* Langford House, Langford, Bristol, BS40 5DU

641 **Table 1. Summary of the Computed Tomography (CT) Settings for all Eighteen**

642 **Dogs**

Patient	CT Scanner†	kV	mAs	Slice Thickness (mm)	Matrix (Size)	DFOV (cm)
1	Siemens Somatom Spirit	130	27	3	512 x 512	30x30
2	Siemens Somatom Spirit	130	32	3	512 x 512	22.4x22.4
3	Siemens Somatom Spirit	130	29	3	512 x 512	16.7x16.7
4	Siemens Somatom Spirit	130	40	3	512 x 512	31.1x31.1
5	GE Medical HighSpeed Dual	120	60	2	512 x 512	13x13
6	GE Brightspeed	120	59	1.3	512 x 512	25x25
7	Philips MX8000 IDT 16	120	129	2	512 x 512	19.6x19.6
8	Philips MX8000 IDT 16	120	122	2	512 x 512	34.9x34.9
9	Toshiba Aquilion Prime	120	100	0.5	512 x 512	20.5x20.5
10	Toshiba Aquilion Prime	120	149	1	512 x 512	25.8x25.8

11	Toshiba Aquilion Prime	120	142	1	512 x 512	22.1x22.1
12	Toshiba Aquilion Prime	120	80	1	512 x 512	31.4x31.4
13	GE Brightspeed	120	72	1.3	512 x 512	23.8 x23.8
14	Siemens Emotion 16	130	24	3	512 x 512	22.3x22.3
15	Philips MX8000 IDT 16	120	162	2	512 x 512	31x31
16	Philips MX8000 IDT 16	120	138	2	512 x 512	19.6x19.6
17	GE Medical HighSpeed Dual	120	43	2	512x512	13x13
18	GE Medical HighSpeed Dual	120	115	5	512x512	20.2x20.2

643

644

645 **Table 2. Criteria Used to Classify Thoracic CT Findings in 18 Dogs.**

Classification Group	Features
0	No changes noted
1 (Mild)	Some or all zones affected, with predominately ground –glass opacity with only occasional areas of consolidation noted.
2 (Moderate)	All zones are affected, with multifocal areas of mixed attenuation (ground –glass opacity and mosaic attenuation) change affecting multiple, if not all, lobes. There is the occasional areas of consolidation observed.
3 (Severe)	Multiple areas to diffuse changes in all zones with clear areas of marked hyperattenuation and consolidation resulting in loss of vascular margins. This is accompanied by marked ground-glass opacity. There may be co-existing features of bronchiectasis or air-trapping resulting in a mosaic attenuation pattern.

646

647 **Appendix 1. Summary of Patient Data (N=18).**

Dog	Age (months)	Breed	Gender	Weight (kg)	Presenting complaint	Onset	CT Severity score
1	3	Gold Retriever	F	13	Respiratory signs	Acute	3
2	5	WHWT	M	3.4	Respiratory signs	Acute	3
3	21	Dachshund	FN	5.8	Respiratory signs	Chronic	2
4	35	Mini Schnauzer	MN	12.3	Respiratory signs	Chronic	3
5	66	Cocker Spaniel	M	14	Respiratory signs	Chronic	3
6	71	Basset Hound	F	22.4	Respiratory signs	Chronic	2
7	75	Dalmatian	M	36.1	Respiratory signs	Chronic	3
8	80	CKCS	MN	15	Neurological, Respiratory signs	Chronic	2
9	84	Greyhound	MN	27	Respiratory signs, Bleeding diathesis	Acute	1
10	89	Mini Schnauzer	FN	7.7	Respiratory signs	Acute	2
11	94	Gold Retriever	FN	34.4	Respiratory signs	Chronic	2
12	95	Gold Retriever	MN	27	Respiratory signs	Chronic	2
13	100	Lurcher	FN	27.2	Neurological, bleeding diathesis	Acute	1
14	119	SBT X	M	15.1	Neurological	Chronic	2
15	121	Lab Retriever	FN	27.9	Respiratory signs	Acute	3
16	129	SBT	M	17.2	Respiratory signs	Chronic	3
17	140	Lab Retriever	M	42.5	Respiratory signs	Chronic	3
18	148	Gold Retriever	F	26.2	Bleeding diathesis	Chronic	1

648

Figure legends

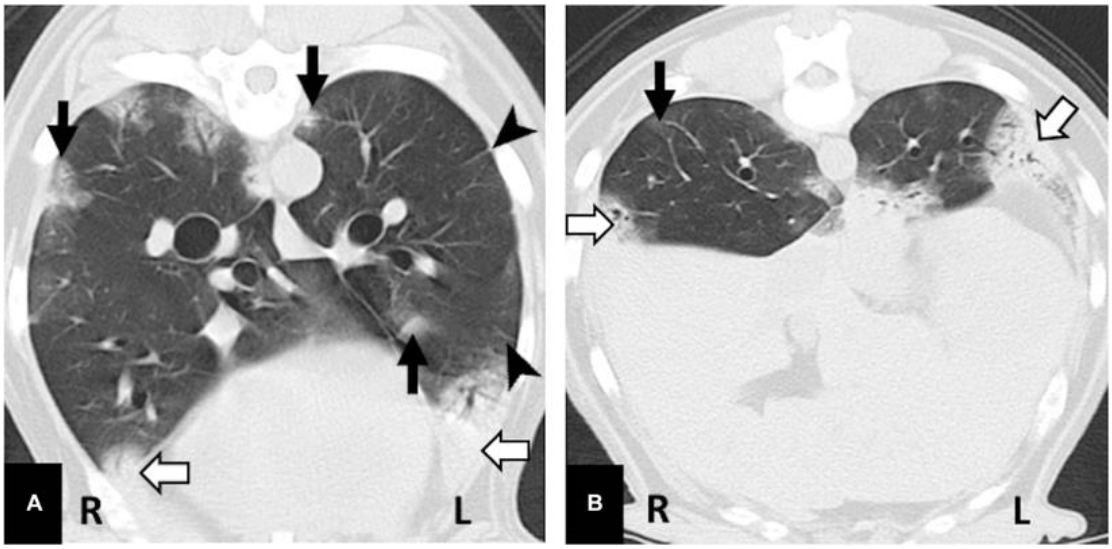

Fig. 1 Transverse CT image of the thorax of a dog infected with *A. vasorum* obtained at the level of the right and left caudal lobes, and also includes the right accessory lung lobe (A). The caudal thorax is shown with the right and left caudal lung lobes given a score of 1 demonstrating mild parenchymal lesions (B). There are prominent parenchymal bands extending from the zone 1 into zone 2, with increased attenuation on the periphery of the lobe (black arrow head). Areas of patchy soft tissue attenuation resulting in effacement of the pulmonary vasculature, suggesting consolidation, are identifiable ventrally and in the caudal lung field; this is identifiable in both the left and right hemithorax (white arrow). Atelectasis (pertaining to cicatrisation, compression or dependent) may be considered as a possible cause of the radio-pathological sign. There is an ill-defined area of increased attenuation (GGO) within zone 2 and zone 3 (black arrow). There is a degree of bronchiolectasis identified in the left caudal lobe, seen in the peribronchovascular and subpleural zones. Window width (WW) 1400, window Level (WL) -500.

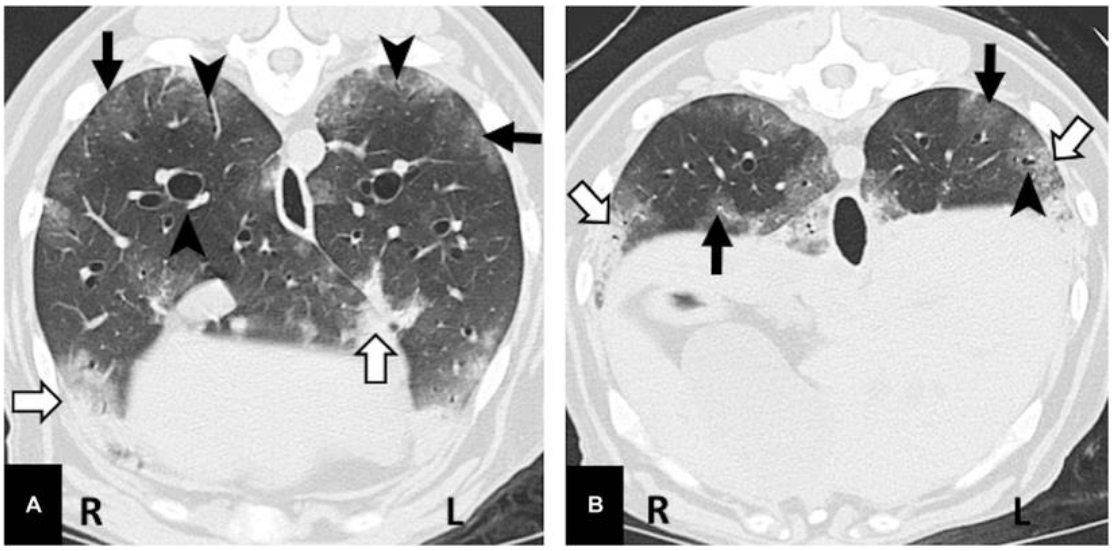

Fig. 2 Transverse CT images of the lungs of a dog at the level of the right accessory lung lobe (A) and the right caudal and left caudal lung lobes (B), given a score of 2 (moderate changes). All lung lobes are affected, with lesions most notable in the peripheral regions (zone 1 and 2). There is rare central involvement (zone 3). There was mosaic attenuation with multifocal regions of GGO (black arrow) and parenchymal consolidation (white arrow). Mild to moderate bronchiectasis and bronchiolectasis were diffusely noted and there was subtle subjective peribronchovascular thickening (peribronchial cuffing) denoted by the *black arrow head*. The ventral and caudal portions of the right and left caudal lobes are affected with the central region (zone 3) spared. WW/WL 1400/-500.

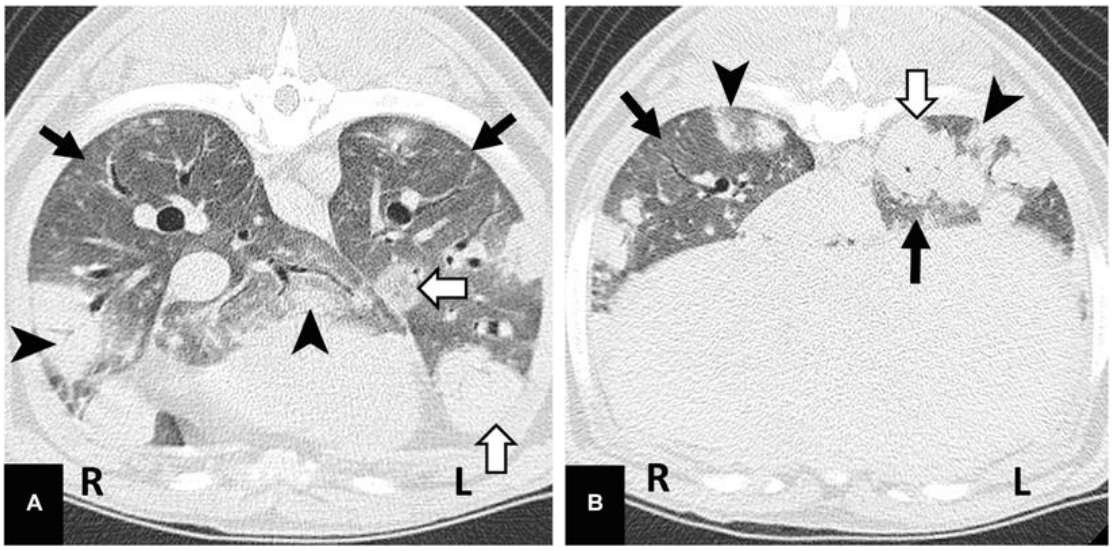

Fig. 3 Transverse CT image of the thorax of a dog naturally infected with *A. vasorum* and given a severity score 3 (severe) showing the level of the accessory, right middle and caudal and left caudal lobes (A) and at the level of the caudal area of the caudal lobes (B). The increased opacity of the lung lobes may be due to anesthesia induced atelectasis, underlying pathology or a combination of both. The most prominent lesions are multifocal areas of coalescing consolidation within the zone 2 and zone 3 (arrow heads); this appears base wide at the pleura. There are ill-defined to well circumscribed, heterogeneous hyper attenuating nodules (-137HU to 36HU) compared to the surrounding parenchyma (white arrows) mean -508HU. All lobes have a diffuse increase in attenuation (black arrows) with severe, diffuse consolidation (soft tissue attenuation). The right middle is severely affected. WW/WL 1400/-500.

Appendix 1: Summary of the presenting signs, signalment and severity score for CT findings for each of the 18 dogs.

Abbreviations: M, male; F, female; MN, male neutered; FN, female neutered; CKCS, Cavalier King Charles Spaniel; Gold Retriever, Golden Retriever; Lab

Retriever, Labrador Retriever; Mini Schnauzer, Miniature Schnauzer; SBT,
Staffordshire Bull Terrier; WHWT, West Highland White Terrier; X, crossbred.